Small-Scale Structure of O VI Interstellar Gas in the Direction of the Globular Cluster NGC 6752[1]

N. Lehner

Department of Astronomy, University of Wisconsin, 475 North Charter Street, Madison, WI 53706

nl@astro.wisc.edu

and

J. C. Howk

Center for Astrophysics and Space Science, University of California, San Diego, C-0424, La Jolla, CA 92093

howk@ucsd.edu

ABSTRACT

In order to study the small-scale structure of the hot interstellar gas, we obtained *Far Ultraviolet Spectroscopic Explorer* interstellar O VI interstellar absorption spectra of 4 four post-extreme horizontal branch stars in the globular cluster NGC 6752 $[(l, b) = (336°50, -25°63)$, $d = 3.9$ kpc, $z = -1.7$ kpc]. The good quality spectra of these stars allow us to measure both lines of the O VI doublet at 1031.926 Å and 1037.617 Å. The close proximity of these stars permits us to probe the hot interstellar gas over angular scale of only $2'.2 - 8'.9$, corresponding to spatial scales $\lesssim 2.5 - 10.1$ pc. On these scales we detect no variations in the O VI column density and velocity distribution. The average column density is $\log\langle N(\text{O VI})\rangle = 14.34 \pm 0.02$ $(\log\langle N_\perp(\text{O VI})\rangle = 13.98)$. The measured velocity dispersions of the O VI absorption are also indistinguishable. Including the earlier results of Howk et al., this study suggests that interstellar O VI is smooth on scales $\Delta\theta \lesssim 12'$, corresponding to a spatial scale of $\lesssim 10$ pc, and quite patchy at larger scales. Although such small scales are only probed in a few directions, this suggests a characteristic size scale for the regions producing collisionally-ionized O VI in the Galaxy.

Subject headings: ISM: clouds – ISM: structure – ultraviolet: ISM

---

1. Introduction

The phase structure of the interstellar medium (ISM) of galaxies is ultimately determined by kinetic and radiative energy input from stars. The heating and ionization of the cold and warm phases of the ISM are principally determined by the effects of stellar UV photons both on atoms and dust grains and the interactions of cosmic rays with the gas (see Wolfire et al. 1995). The hotter phases of the ISM ultimately owe their existence to the injection of energy into the ISM by stellar winds and supernovae.

Hot ($T \sim 10^6$ K), X-ray emitting gas is produced in high-velocity shocks, a process whose basic outline is understood. The subsequent evolution of hot material, including its cooling and interactions with the cooler gas phases, is not well understood. These processes can be probed observationally using resonant absorption lines from lithium-like ions C IV, N V, and O VI, which are produced in collisionally-ionized gas at "coronal temperatures" ($T \sim 10^5$ K; Sutherland & Dopita 1993). These ions have a range of ionization energies, corresponding to a range of temperatures in equilibrium, and all have resonance doublet transitions accessible to modern ultraviolet observatories. Of these, O VI absorption is the most important diagnostic to understanding gas in this temperature regime since it cannot be produced via photoionization in the ISM of galaxies, since the required pathlengths would be too large (see Savage et al. 2003).

Measurements of O VI absorption at high galactic latitudes have accumulated in the recent years via observations with the *Far Ultraviolet Spectroscopic Explorer* (*FUSE*; see Wakker et al. 2003; Savage et al. 2003; Zsargò et al. 2003, and references therein). Spitzer (1956) initially predicted a widespread distribution of hot gas in the Galactic halo in order to confine neutral clouds seen at high latitudes. However, it is clear that the halo as seen in O VI is not the elegant, smooth halo in the idealized models of Spitzer. Instead, the distribution of O VI, while grossly consistent with a thickened layer of hot gas about the Milky Way's disk, is quite complicated (Savage et al. 2003), with a wealth of structure on many scales. Indeed, using *FUSE* observations of a series of closely-spaced early-type stars in the Large and Small Magellanic Clouds (LMC and SMC), Howk et al. (2002a) found large variations in O VI column densities over small angular scales, often finding $\geq 50\%$ variations in N(O VI) between pairs of stars separated by $0°\!\!.3 \lesssim \Delta\theta \lesssim 5°\!\!.0$. This variation on small angular scale extends to large angular scale (Savage et al. 2000, 2003).

However, the spatial/angular structure seen in O VI column densities is potentially providing us with a tool for understanding the physical properties of the regions in which O VI is produced. In particular, the scales of the structures seen in O VI are likely indicating the physical dimensions of typical O VI regions, while an analysis of the amount of change in N(O VI) and the size scale of variations could lead to information about the topology of the O VI-bearing structures.

The results of Howk et al. (2002a) have, to date, been the only thorough analysis of the structure of O VI on small scales. They found column density variations on even the smallest scales they were able to probe, $\Delta\theta \sim 1'\!\!.8$, although their dataset included only two pairs of sight lines with separations $< 10'$.

To investigate the structure of O VI on smaller angular scales, we have obtained *FUSE* spectra of four post-extreme horizontal branch (post-EHB) stars in the globular cluster NGC 6752 $[(l,b) = (336°50, −25°63), d = 3.9$ kpc, $z = −1.7$ kpc, Harris 1996]. Figure 1 shows a NUV image ($\lambda_c = 1620$ Å) of NGC 6752 obtained with the *Ultraviolet Imaging Telescope* by Landsman et al. (1996) during the Astro-2 mission of the Space Shuttle *Endeavour* in 1995. We have marked our four post-EHB targets, indicating the angular separations (in arcminutes) between each pair. For reference 1′ is about 1 pc at the distance of NGC 6752.

The choice of stars in a single globular cluster allows us to probe the degree of variation in the coronal temperature gas over small angular ($2′2 − 8′9$) and spatial ($\lesssim 2.5 − 10.1$ pc) scales. Furthermore, the choice of hot, highly-evolved globular cluster stars is important: such stars have proven to provide the least complicated stellar continua in the regions near interstellar O VI (Howk, Sembach, & Savage 2003), allowing very accurate column density determinations. Indeed, population I OB-type stars, such as those used as background sources in the LMC and SMC, can have quite complex (and even temporally variable) continua in the regions near interstellar O VI due to their out-flowing stellar winds (Lehner et al. 2001; Howk et al. 2002b; Hoopes et al. 2002). The current study avoids this source of uncertainty.

In the remainder of the paper, we will present the observations (§ 2) and analysis (§ 3) of the *FUSE* O VI data, demonstrating that there is no detectable variability in N(O VI) between our four sight lines. In § 4, we discuss the implications of our measurements, and compare them with the previous study of Howk et al. (2002a). Lastly, we present concluding remarks in § 5.

2.   *FUSE* Observations and Data Reduction

We obtained far-ultraviolet spectra of our four target post-EHB stars using *FUSE*, which is described in detail by Moos et al. (2000); Sahnow et al. (2000), in 2002 April and June as part of the GI program C076 (PI: Howk). The basic parameters of the observations are summarized in Table 1, including pertinent information about our target stars. Each target was observed using the MDRS ($4″ \times 20″$) apertures with the detectors in photon-address, or time-tag (TTAG), mode. The MDRS apertures were used with roll angle constraints to exclude other stars in NGC 6752 that could potentially contaminate our spectra. The resolution of the data is $R \sim 15,000$, or $\Delta v \sim 20$ km s^{-1}.

The *FUSE* instrument has four channels: two optimized for the short wavelengths (SiC 1 and SiC 2; 905–1100 Å) and two optimized for longer wavelengths (LiF 1 and LiF 2; 1000–1187 Å). The wavelength overlap of the various channels is important for identifying potential fixed-pattern noise in the data. For three of our datasets, only the LiF channels were aligned at the time of the observations, providing us with coverage longward of 1000 Å. For NGC 6752-B852, the SiC channels were aligned as well, providing full wavelength coverage. The lack of full wavelength coverage for three of our stars does not affect our scientific goals since the effective areas of the LiF channels is

much higher than the SiC channels at O VI (1031.926 and 1037.617 Å).

We used the standard calibration pipeline software (CalFUSE version 2.1.6) to extract and calibrate the spectra. The software screened the data for valid photon events, removed burst events, corrected for geometrical distortions, spectral motions, satellite orbital motions, and detector background noise, and finally applied flux and wavelength calibrations. The extracted spectra associated with the separate exposures were aligned by cross-correlating the positions of interstellar absorption lines, and then co-added. The co-added spectra were finally rebinned by 4 pixels (~ 27 mÅ) since the extracted data are oversampled. This provides approximately three samples per 20 $\mathrm{km\,s^{-1}}$ resolution element. In Figure 2 we show the final spectra of our stars near the location of interstellar O VI.

The reference frame for the *FUSE* wavelength is heliocentric. Toward this direction $v_{\mathrm{helio}} \simeq v_{\mathrm{LSR}}$, where v_{LSR} is the local standard of rest (LSR) velocity. Since the *FUSE* absolute wavelength zero point is quite uncertain, we use the known radial velocity of NGC 6752 at -24.4 $\mathrm{km\,s^{-1}}$ (Harris 1996), and we assume that the 4 observed stars have this radial velocity. We use identified and uncontaminated stellar lines (P IV $\lambda\lambda1030.515, 1033.112$) to correct the velocity. In Figure 3, we show the normalized spectra (see § 3) against the LSR velocity. There is a good agreement of the cloud velocity toward the 4 stars. The mean centroid velocity for P II and Fe II interstellar clouds is $+9.8 \pm 4.2 \pm 5$ $\mathrm{km\,s^{-1}}$, where ±4.2 $\mathrm{km\,s^{-1}}$ is the dispersion around the mean, and ±5 $\mathrm{km\,s^{-1}}$ the adopted relative velocity accuracy. We note, however, that the rotation curve of Clemens (1985) for the direction of NGC 6752 predicts LSR radial velocities between -45 to 0 $\mathrm{km\,s^{-1}}$ for clouds at distance $d \lesssim 4$ kpc.

3. Analysis

3.1. Continuum Placement

While the continuum placement can be very difficult to determine in early-type stars and can remain uncertain especially near the interstellar O VI absorption because of the strong O VI winds in those stars (Lehner et al. 2001; Howk et al. 2002b; Zsargó et al. 2003), this is not a concern for post-EHB stars. The calibrated spectra of our four targets in the region of the interstellar O VI doublet are shown in Figure 2. We identify the main absorption lines from atomic and ionic species as well as molecular hydrogen above the top spectrum. All unmarked absorption lines are photospheric. NGC 6752-UIT-1 obviously shows the most metal lines in our sample, and these will be a source of contamination for our $N(\mathrm{O\,VI})$ measurements. The dotted lines show our adopted continua, modeled as first order Legendre polynomials, are very good matches to the line-free regions of these spectra.

3.2. Column Density Measurements

The O VI absorption line is broad enough to be fully resolved by *FUSE*. We therefore use the apparent optical depth described by Savage & Sembach (1991). In this method, the absorption profiles are converted into apparent optical depth (AOD) per unit velocity, $\tau_a(v) = \ln[I_c/I_{\mathrm{obs}}(v)]$, where I_{obs}, I_c are the intensity with and without the absorption, respectively. The AOD, $\tau_a(v)$, is related to the apparent column density per unit velocity, $N_a(v)$, through the relation

$$N_a(v) = 3.768 \times 10^{14} \frac{\tau_a(v)}{f\lambda(\text{Å})} \ \mathrm{cm}^{-2}\,(\mathrm{km\,s}^{-1})^{-1}. \tag{1}$$

The integrated apparent column density is equivalent to the true integrated column density when the lines are fully resolved. In Figure 4, we show the apparent column density comparison of the O VI doublet for our four target stars. The $N_a(v)$ profiles for NGC 6752-UIT-1 indicates some blending of O VI $\lambda 1032$, possibly with a stellar absorption line at $+15\ \mathrm{km\,s}^{-1}$. Except for this sight line, there is an excellent agreement between $N_a(v)$ for the two O VI absorption lines, implying that the two lines contain no unresolved saturated structure and that there is no contamination from stellar lines or the HD 6–0 R(0) absorption line at 1031.912 Å. (We nevertheless checked that the HD line at 1066.271 Å was not present in our spectra to insure our O VI profiles were not contaminated by HD.)

The total column density is obtained by integrating the profile, $N = \int N_a(v)dv$, between the velocity range $[-v, +v]$. The results are shown in Table 2, and again one can see the very good agreement between the column density from O VI $\lambda 1032$ and O VI $\lambda 1038$, except for O VI $\lambda 1032$ toward NGC 6752-UIT-1, which is too large. In Table 3, the adopted average column densities of the two O VI lines are indicated (with the value for NGC 6752-UIT-1 from O VI $\lambda 1038$ only).

For comparison between the highly ionized gas and neutral and weakly ionized gas, we also measure the column densities of P II and Fe II. Many accessible lines exist for Fe II, but several are contaminated by stellar lines. We selected the weakest Fe II absorption lines that give consistent apparent column densities. Those lines are Fe II $\lambda\lambda 1055$, 1112, and 1143. The choice of these line spans different $f\lambda$, allowing us to check that the lines are not saturated. Within 1σ error, the apparent column densities of these lines are in agreement. For P II, we have only one transition at 1152.818 Å, but recent work by Lehner, Wakker, & Savage (2004) shows that for typically similar velocity distribution and Galactic halo gas probed, this feature suffers little or no saturation.

The quoted uncertainties are 1σ. They contain both statistical (photon noise) and systematic (fixed-pattern noise, continuum placement, velocity range over which the interstellar absorption lines were integrated) contributions added in quadrature.

3.3. Average Velocity and Velocity Dispersion

The average line centroids and the velocity dispersions of O VI are summarized in Table 3. They were estimated using both O VI absorption lines and were computed with the following expressions (Sembach & Savage 1992):

$$\bar{v} = \frac{\int v N_a(v) dv}{\int N_a(v) dv} \ \mathrm{km\,s^{-1}}, \tag{2}$$

$$b = \sqrt{\frac{2 \int (v - \bar{v})^2 N_a(v) dv}{\int N_a(v) dv}} \ \mathrm{km\,s^{-1}}. \tag{3}$$

The quantity b is related to the Doppler parameter used in the Voigt profile fitting of interstellar lines. It contains all the instrumental effects, thermal and turbulent broadening, and is affected by the presence of multiple components.

The 1σ errors listed in Table 3 include statistical (photon counting) and systematic (continuum placement, velocity cutoff) contributions. We have restricted our measurements of the velocity to the LiF 1 channel to avoid spurious velocity shifts that may exist between LiF 1 and LiF 2. The second error of ± 5 km s^{-1} for $\bar{v}$ is the systematic uncertainty from the absolute wavelength scale (see § 2).

The average line centroid of O VI, $+16.0 \pm 5.3 \pm 5$ km s^{-1}, is $\sim +6$ km s^{-1} higher than the average velocity of P II and Fe II, but consistent within 1σ errors (see Figure 2).

4. Discussion: O VI Small-Scale Structure

4.1. Small-Scale Structure Toward NGC 6752

We have presented measurements of O VI column densities toward four stars in the globular cluster NGC 6752. There is good agreement of the O VI column densities, the average line centroids, and the velocity dispersions of O VI along these four sight lines. This is further shown in Figure 5 where the apparent column density of O VI λ1038 toward each sight lines is compared. The sight lines in our study are separated by angular distances of $2' \lesssim \Delta\theta \lesssim 9'$, corresponding to spatial separations of ~ 2 pc to ~ 9 pc at the distance of the globular cluster. The dispersion about the mean column density in this direction is only ± 0.03 dex, or 1.4×10^{13} cm^{-2}. We can limit column density variations between these sight lines to $\Delta N(\mathrm{O\ VI}) \lesssim 8 \times 10^{13}$ cm^{-2} (2σ), or $\Delta N(\mathrm{O\ VI}) \lesssim 4 \times 10^{13}$ cm^{-2} (2σ) if we exclude NGC 6752-UIT-1 (in case weak stellar lines contaminate the O VI 1037.617 Å transition).

Our data also show the kinematics of the absorption along each of these sight lines to be indistinguishable. In short, there is no evidence that we are probing any differences in the properties

of the O VI-bearing gas as we compare these four sight lines. Neither the column densities nor the kinematics of O VI toward NGC 6752 are peculiar with respect to other sight lines at similar galactic latitudes (see Savage et al. 2003).

The low ions (P II and Fe II) also show no evidence for column density variations among the four sight lines studied in this work. Concerns about unresolved saturation in these profiles makes the limits on relative variations in these species larger (i.e., less constraining). The P II and Fe II are significantly narrower than the O VI profiles along these sight lines. This is likely in part due to the different temperatures of gas probed by these species. However, it should be noted that the profiles of the strongest low-ion absorption lines in the *FUSE* data, such as the strongly-saturated C II 1036.337 Å transition, have the same total breadth (defined as the approximate velocities at which the absorption profiles return to the continuum) as O VI. This could imply that the O VI absorption is arising in interfaces between hotter and cooler gas, with the total amount of O VI as a function of velocity indicating the relative number of interfaces in each velocity range.

Absorption from the low ions is clearly (and expectedly) tracing different material along these sight lines, given the very different kinematic properties compared to the O VI absorption. The O VI profiles are clearly more extended than the profiles of the low ions (see Figure 3), implying that O VI absorption contains more and/or broader components than the low ions.

While we see no evidence for variations in O VI column densities over the $\lesssim 9'$ angular scales probed by the current observations, there is evidence for variations over larger scales in this region of the sky. Savage et al. (2003) report on *FUSE* observations of the AGN ESO 141-G55, some $1°.8$ from the center of NGC 6752. They derive an O VI column density of $\log N(\mathrm{O\,VI}) = 14.50 \pm 0.02 \pm 0.02$ (random and systematic uncertainties, respectively) toward ESO 141-G55, +0.16 dex larger than toward NGC 6752. This could be a signature of significant O VI at distances greater than that of NGC 6752; indeed, if the scale-height of O VI is ~ 2.3 kpc (Savage et al. 2003), then this cluster may only reside behind $\sim 50\%$ of the total O VI column density in this direction.

4.2. Comparison with the LMC and SMC Lines of Sight

Howk et al. (2002a) presented observations of Galactic O VI absorption toward 23 stars in the Magellanic Clouds drawn from the sight lines studied by Howk et al. (2002b) (for the LMC) and Hoopes et al. (2002) (for the SMC). The angular separations of the observed stars range from $\sim 3'.0$ to $\sim 5°.0$. Most of the sight lines studied by Howk et al. in the LMC were separated by much larger angular scales than those toward NGC 6752, with a minimum angular separation of $\approx 30'$. The angular separations of the sample of stars studied in the SMC is closer to those in the current sample. The smallest separations studied toward the SMC were $3'.0$, $9'.1$, $10'.5$. Thus, the smallest separations were on scales similar to those studied in this work. Assuming the bulk of the O VI in these directions resides within two vertical scale heights, i.e., $z_{O\,VI} \lesssim 2h_z$ 5.0 kpc (Savage et al. 2003), the corresponding spatial scales probed by these observations are $\ll 80$–800 pc toward the

LMC and $\ll$ 6–400 pc (Howk et al. 2002a).

O VI column density variations were seen over effectively all scales probed. Typical variations were in the range $\sim 25\%$ to $\sim 50\%$, although there were pairings of sight lines with much smaller variations (consistent with no change) and larger variations (up to a factor of 4 variation between sight lines separated by $1°$ to $2°$). Howk et al. (2002a) discuss the angular correlation function of the O VI measurements, finding no preferred angular scale for the O VI variations. Savage et al. (2003) showed that the variations seen toward the LMC and SMC extend to larger angular scales. On smaller angular scales, Danforth et al. (2002) have reported a lack of column density variations greater than $\sim 12\%$ toward several stars in the SMC cluster NGC 346 with an average separation of $\lesssim 19''$. Thus, the SMC observations suggest the O VI is smooth on scales less than an arcminute and patchy on slightly larger scales.

The lack of O VI column density variations in the current study on scales as small as those identified toward the SMC, may be due to the different sight lines these two samples probe through the Galactic ISM. However, there are two concerns that should be mentioned regarding the Magellanic Cloud measurements that are not existing toward NGC 6752, and both of which are probably more extreme for the SMC sight lines. First, the stellar continua in the region of interstellar O VI are quite complex for the early-type stars used to probe the Magellanic Clouds. Howk et al. (2002b) and Hoopes et al. (2002) discuss in detail the difficulties of accurately determining a continuum in the face of these complexities. The variations claimed over angular scale of $3'.0$ by Howk et al. (2002a) are potentially susceptible to systematic uncertainties associated with the placement of the stellar continuum. We believe the SMC measurements would be more likely to suffer from this source of systematic error given the stellar winds that dominate the shape of the stellar continuum in this wavelength region are significantly better developed and well behaved in the LMC. Indeed, among the closest pairing of stars in the SMC, the direction toward Av 83 has a much smaller O VI column density (13.93 dex) than toward two nearby directions (Av 75 and Av 95, with $\log N(\text{O VI}) = 14.15$ and 14.14, respectively), but the stellar continua of these stars are among the least certain in the sample of Hoopes et al. (2002). The continuum for Av 83 is especially difficult. If the latter star is removed from the sample, the smallest scale in Howk et al. (2002a) over which O VI variations are seen would be $\sim 10'$. Reexamining the data for Av 83, we favor this scenario. The problems associated with stellar continuum placement uncertainties are not applicable to the NGC 6752 sight lines given the nature of the observed stars (see Figure 2).

Another possible source of systematic error for Milky Way measurements in the Magellanic Cloud directions is the presence of material flowing out of these galaxies with velocities that overlap the expected Milky Way velocities or intermediate-velocity gas not well separated from the Galactic halo gas (Hoopes et al. 2001; Lehner, Keenan, & Sembach 2001; Danforth et al. 2003). For the SMC the outflow velocities required are ~ 150 km s^{-1}; for the LMC, the outflow velocities required are $\gtrsim 200$ km s^{-1}. Thus, it seems more likely that this effect would contaminate directions toward the SMC. Hoopes et al. (2001) have reported on the detection of the receding side of a supernova remnant in O VI toward the SMC star HD 5980. The analysis of Danforth et al. (2003) suggested

that the approaching side of the shell may overlap the low-velocity Milky Way O VI toward stars projected onto the remnant. Their measurements showed the Milky Way O VI to be stronger in directions toward the remnant than those several arcminutes outside the remnant. Unfortunately this result could imply either that arcminute variations in the Galactic halo O VI are seen in this direction, or that the approaching side of the remnant is contaminating the Milky Way gas.

It is tempting to repeat the analysis of the O VI angular correlation function discussed by Howk et al., including the current measurements. However, the likelihood that the sight line to NGC 6752 only probes a fraction of the total O VI integrated through the Galaxy, while the Howk et al. data extend through the entire halo, makes this seem like a somewhat dubious endeavor.

5.   Concluding Remarks

We have presented observations of Galactic halo O VI absorption toward 4 post-EHB stars in NGC 6752 situated at a distance of 3.9 kpc and separated by only $2.'2 - 8.'9$ allowing to study the hot interstellar gas on small spatial scales of $\lesssim 2.5 - 10.1$ pc. The continuum of these stars is well behaved and we were able to derive accurate O VI measurements.

A comparison of the present results with the results of Howk et al. (2002a) toward the LMC and SMC and the results of Danforth et al. (2002) toward the SMC cluster NGC 346 shows that there is a higher frequency of $N(\text{O VI})$ variations on degree-scale separation greater than $\Delta\theta \gtrsim 30'$. On degree-scale separation smaller than $\Delta\theta \lesssim 12'$ corresponding to spatial-scale separation $\lesssim 10$ pc, O VI is more smoothly distributed and does not have the complexity of the larger-scale distribution.

Howk et al. (2002a) and Savage et al. (2003) discussed the existence of large column density variations over various angular scale favored models in which the O VI-bearing medium is composed of small complex cloud-like or sheet-like distributions of material (such envisioned in various interface models), rather than models in which O VI is distributed in a diffuse, smooth medium. If O VI is in small complex clouds, these clouds cannot generally be smaller than 10 pc in the direction of NGC 6752 unless we are seeing these structures in a face-on orientation.

REFERENCES

Clemens, D. P. 1985, ApJ, 295, 422

Danforth, C. W., Howk, J. C., Fullerton, A. W., Blair, W. P., & Sembach, K. R. 2002, ApJS, 139, 81

Danforth, C. W., Sankrit, R., Blair, W. P., Howk, J. C., & Chu, Y. 2003, ApJ, 586, 1179

Harris, W. E. 1996, AJ, 112, 1487

Hoopes, C. G., Sembach, K. R., Howk, J. C., & Blair, W. P. 2001, ApJ, 558, L35

Hoopes, C. G., Sembach, K. R., Howk, J. C., Savage, B. D., & Fullerton, A. W. 2002, ApJ, 569, 233

Howk, J. C., Savage, B. D., Sembach, K. R., & Hoopes, C. G. 2002a, ApJ, 572, 264

Howk, J. C., Sembach, K. R., Savage, B. D., Massa, D., Friedman, S. D., & Fullerton, A. W. 2002b, ApJ, 569, 214

Howk, J. C., Sembach, K. R., & Savage, B. D. 2003, ApJ, 586, 249

Landsman, W. B., Sweigart, A. V., Bohlin, R. C., Neff, S. G., O'Connell, R. W., Roberts, M. S., Smith, A. M., & Stecher, T. P. 1996, ApJ, 472, L93

Lehner, N., Fullerton, A. W., Sembach, K. R., Massa, D. L., & Jenkins, E. B. 2001, ApJ, 556, L103

Lehner, N., Keenan, F. P., & Sembach, K. R. 2001, MNRAS, 323, 904

Lehner, N, Wakker, B. P., & Savage, B. D., 2004, ApJ, in press (astro-ph/0407363)

Moos, H.W., et al. 2000, ApJ, 538, L1

Sutherland, R.S., & Dopita, M.A. 1993, ApJS, 88, 253

Savage, B. D., & Sembach, K. R. 1991, ApJ, 379, 245

Savage, B. D. et al. 2000, ApJ, 538, L27

Savage, B. D., et al. 2003, ApJS, 146, 125

Sahnow, D. J., et al. 2000, ApJ, 538, L7

Sembach, K. R., & Savage, B. D. 1992, ApJS, 83, 147

Spitzer, L. J. 1956, ApJ, 124, 20

Wakker, B. P., et al. 2003, ApJS, 146, 1

Wolfire, M. G., Hollenbach, D., McKee, C. F., Tielens, A. G. G. M., & Bakes, E. L. O. 1995, ApJ, 443, 152

Zsargó, J., Sembach, K. R., Howk, J. C., & Savage, B. D. 2003, ApJ, 586, 1019

– 11 –

Table 1.   Observation Summary

Object	R.A. (h m s)	Dec. (∘ ’ ”)	l (∘)	b (∘)	$t_{\exp}$ (ks)	S/N	ID	Observation Date
NGC 6752-UIT-1	19 10 54.50	−59 59 46.40	336.48	−25.64	30.3	11	C0760101	Apr. 10 2002
NGC 6752-B2004	19 11 04.78	−59 57 59.19	336.52	−25.65	38.1	10	C0760201	Jun. 04 2002
NGC 6752-B852	19 11 27.89	−60 00 39.10	336.48	−25.71	34.9	12	C0760301	Apr. 14 2002
NGC 6752-B1754	19 11 08.87	−59 52 20.70	336.62	−25.64	36.7	14	C0760401	Apr. 15 2002

Note. — Typical signal-to-noise (S/N) may fluctuate slightly depending on which wavelength range is studied. The S/N is per ∼27 mÅ binned pixel.

Table 2.   Colum Densities

Ions	NGC 6752-UIT-1 $\log N \, [-v, +v]$ (cm^{-2}, km s^{-1})	NGC 6752-B2004 $\log N \, [-v, +v]$ (cm^{-2}, km s^{-1})	NGC 6752-B852 $\log N \, [-v, +v]$ (cm^{-2}, km s^{-1})	NGC 6752-B1754 $\log N \, [-v, +v]$ (cm^{-2}, km s^{-1})
O VI λ1032	14.47 ± 0.04 [−56, +84]	14.36 ± 0.05 [−44, +68]	14.33 ± 0.04 [−43, +92]	14.34 ± 0.02 [−45, +88]
O VI λ1038	14.39 ± 0.06 [−56, +84]	14.34 ± 0.06 [−44, +68]	14.35 ± 0.04 [−43, +92]	14.33 ± 0.03 [−45, +88]
P II λ1152	13.75 ± 0.06 [−11, +34]	13.66 ± 0.10 [−15, +30]	13.65 ± 0.04 [−6, +36]	13.66 ± 0.04 [−9, +35]
Fe II	14.80 ± 0.07 [−11, +34]	14.82 ± 0.10 [−15, +30]	14.80 ± 0.07 [−6, +36]	14.80 ± 0.02 [−9, +35]

Note. — The Fe II measurements result from 3 absorption lines at 1055 Å, 1112 Å, and 1143 Å. Toward NGC 6752-UIT-1, O VI λ1032 is contaminated by a stellar line, and another stellar line possibly contaminates also P II λ1152.

Table 3.   Adopted Column Densities, Line Widths, and Velocities of O VI Absorption

Target	$\log N$ (dex)	$\log(N \sin |b|)$ (dex)	b (km s^{-1})	$\bar{v}_{\rm LSR}$ (km s^{-1})
NGC 6752-UIT-1	14.39 ± 0.06	14.03 ± 0.06	42.4 ± 4.5	+11.8 ± 5.8 ± 5.0
NGC 6752-B2004	14.35 ± 0.04	13.99 ± 0.04	42.4 ± 2.2	+11.3 ± 3.0 ± 5.0
NGC 6752-B852	14.34 ± 0.03	13.98 ± 0.03	43.3 ± 1.6	+22.0 ± 2.7 ± 5.0
NGC 6752-B1754	14.34 ± 0.02	13.98 ± 0.02	42.5 ± 1.1	+18.9 ± 2.0 ± 5.0

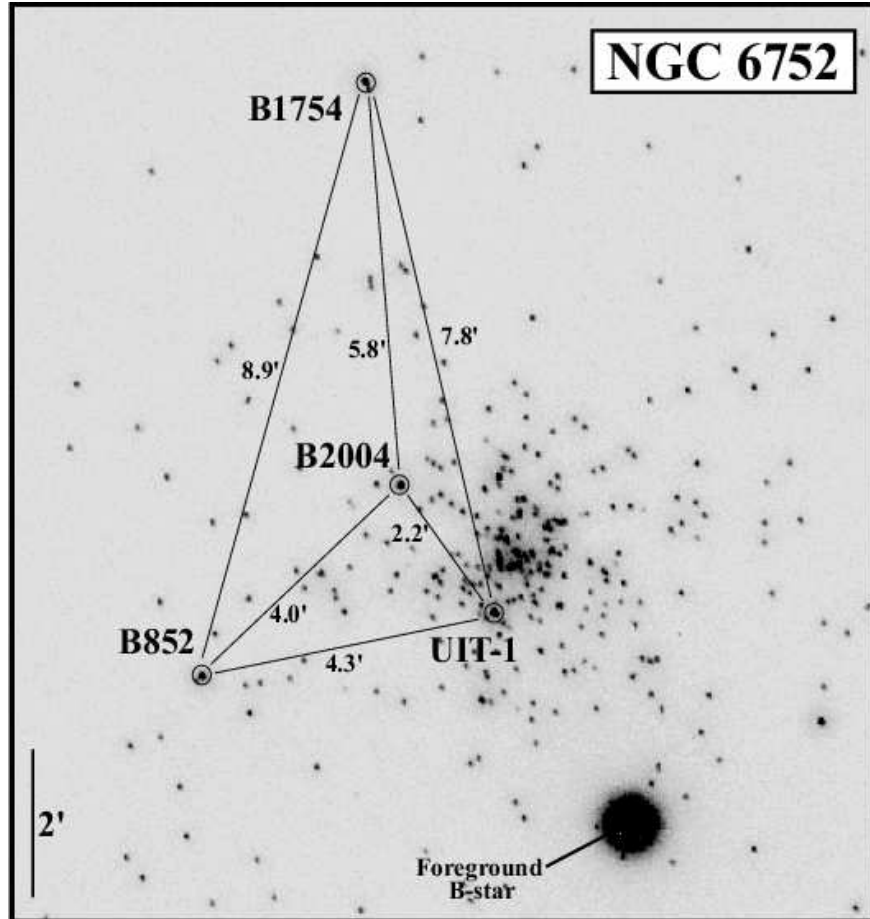Fig. 1.— The NUV ($\lambda_c = 1620$ Å) UIT image of NGC 6752 with our background post-EHB stars marked. The separation of these stars are marked, where $1' \simeq 1$ pc at the distance of 3.9 kpc of the globular cluster. All these stars were observed in the MRDS ($4'' \times 20''$) aperture of *FUSE* to exclude fainter stars that could contaminate our spectra.
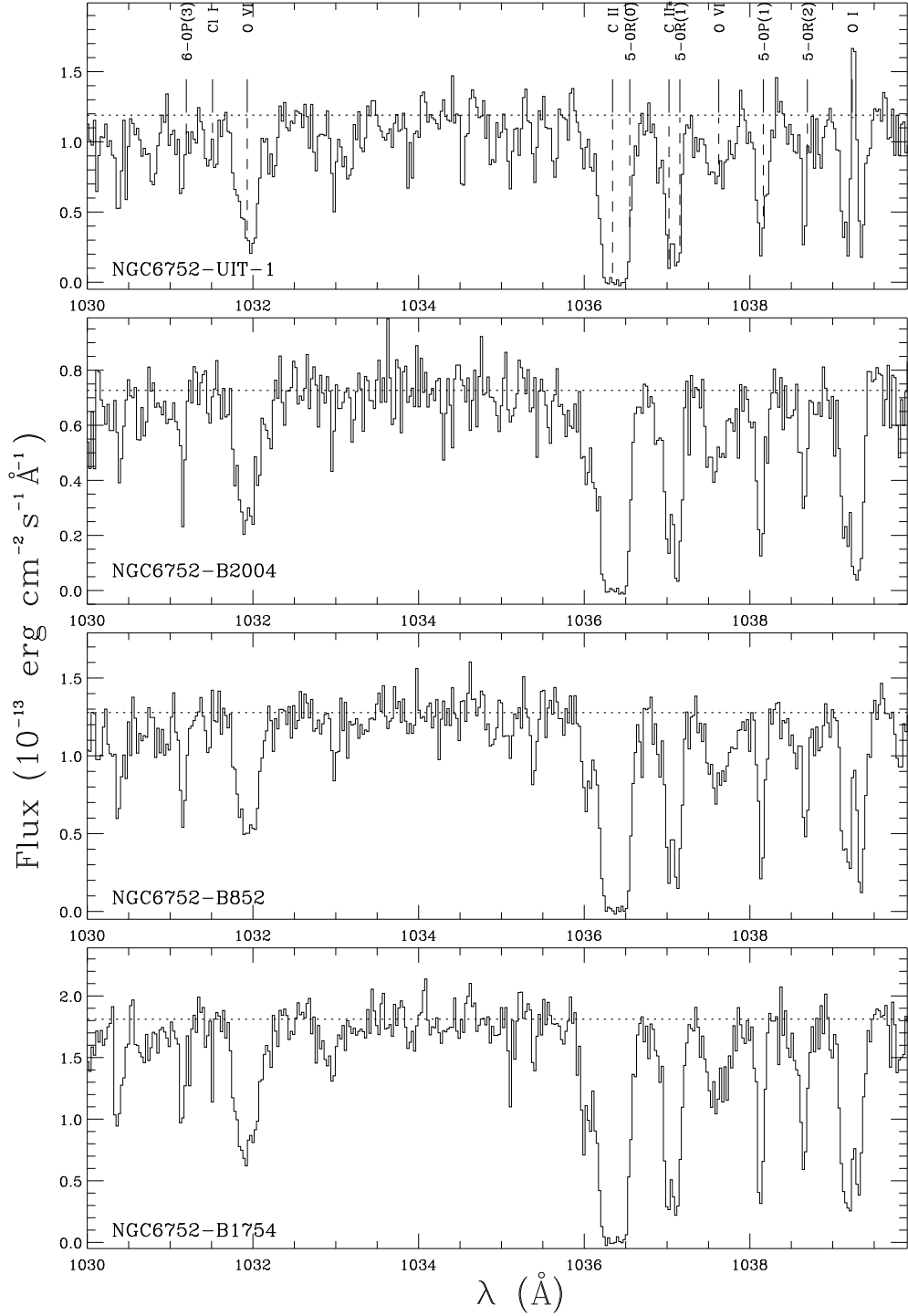
Fig. 2.— Spectra of the different line of sights. The dotted line indicates the stellar continuum. In the top diagram, we indicate the main interstellar (atomic, ionic, hydrogen molecular) absorption, and in particular the O VI doublet.
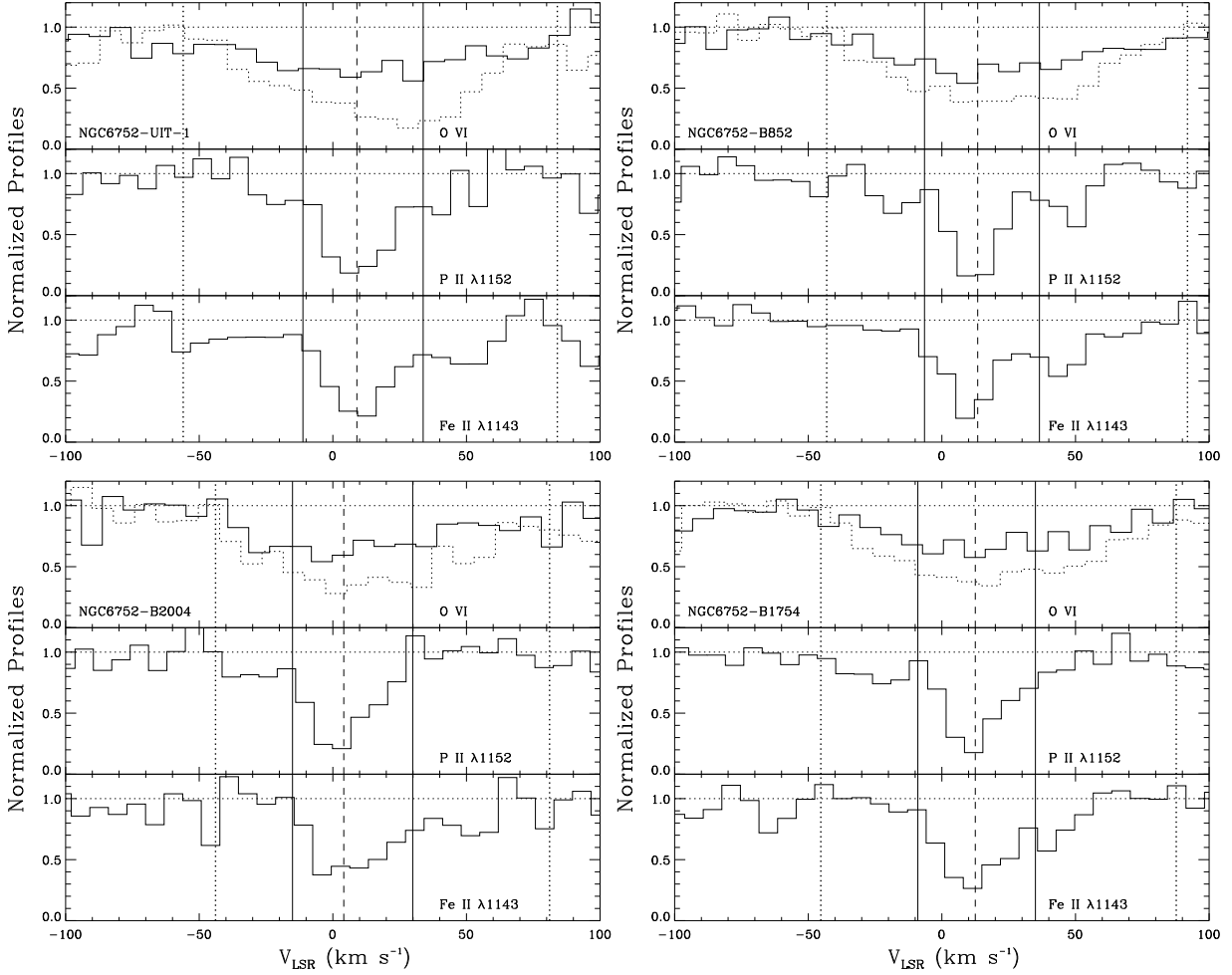
Fig. 3.— Normalized profiles versus the velocity. For O VI, the lines at $\lambda1032$ (dotted line) and $\lambda1038$ (solid line) are shown. The vertical dotted lines indicate the extent of the O VI absorption profile. The vertical solid lines indicate the low ions extent (anything outside this two lines are stellar lines). The dashed line represent the centroid of low ions; the typical uncertainty on this point is $\sim \pm8$ km s^{-1} (including the statistic and systematic uncertainties).
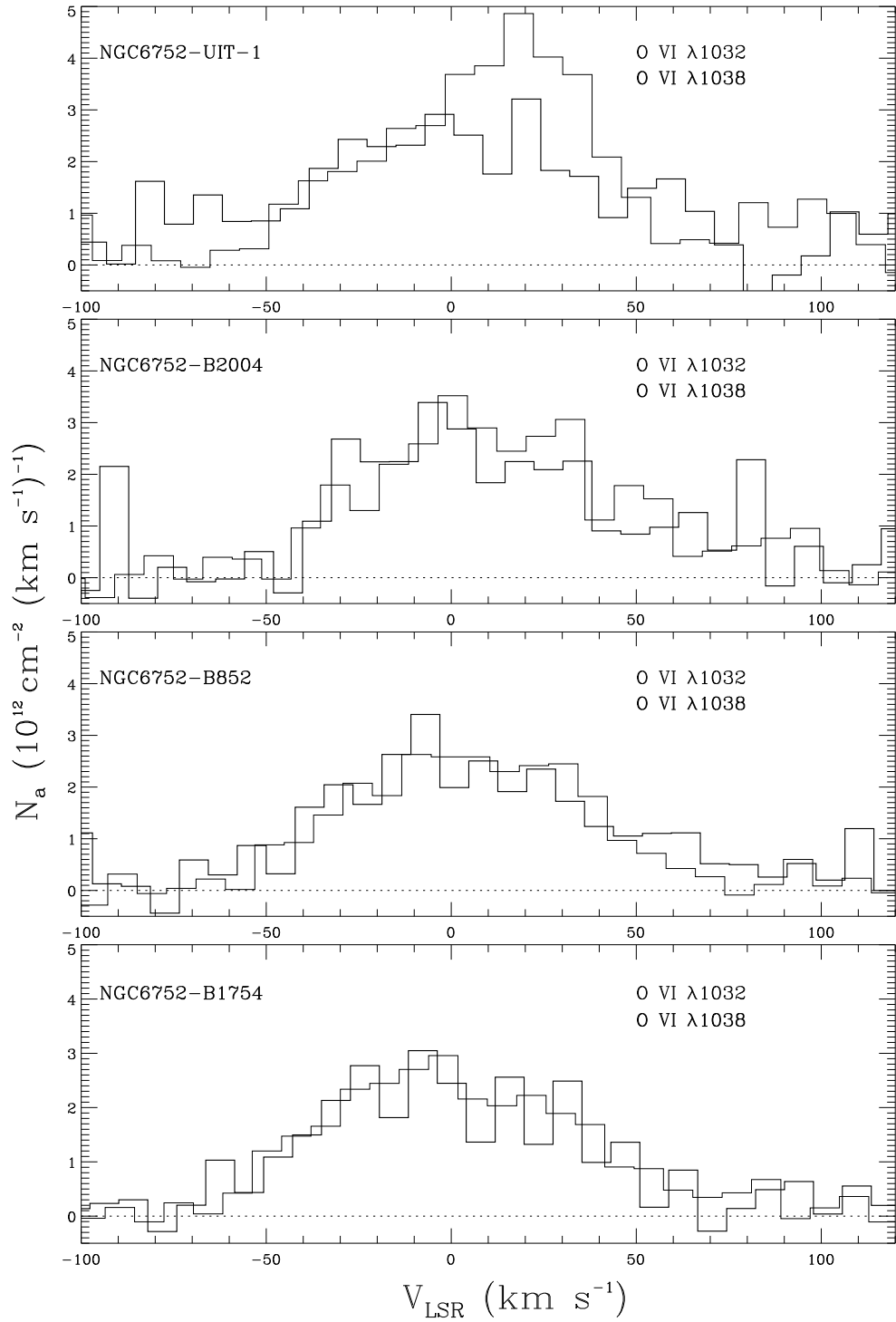
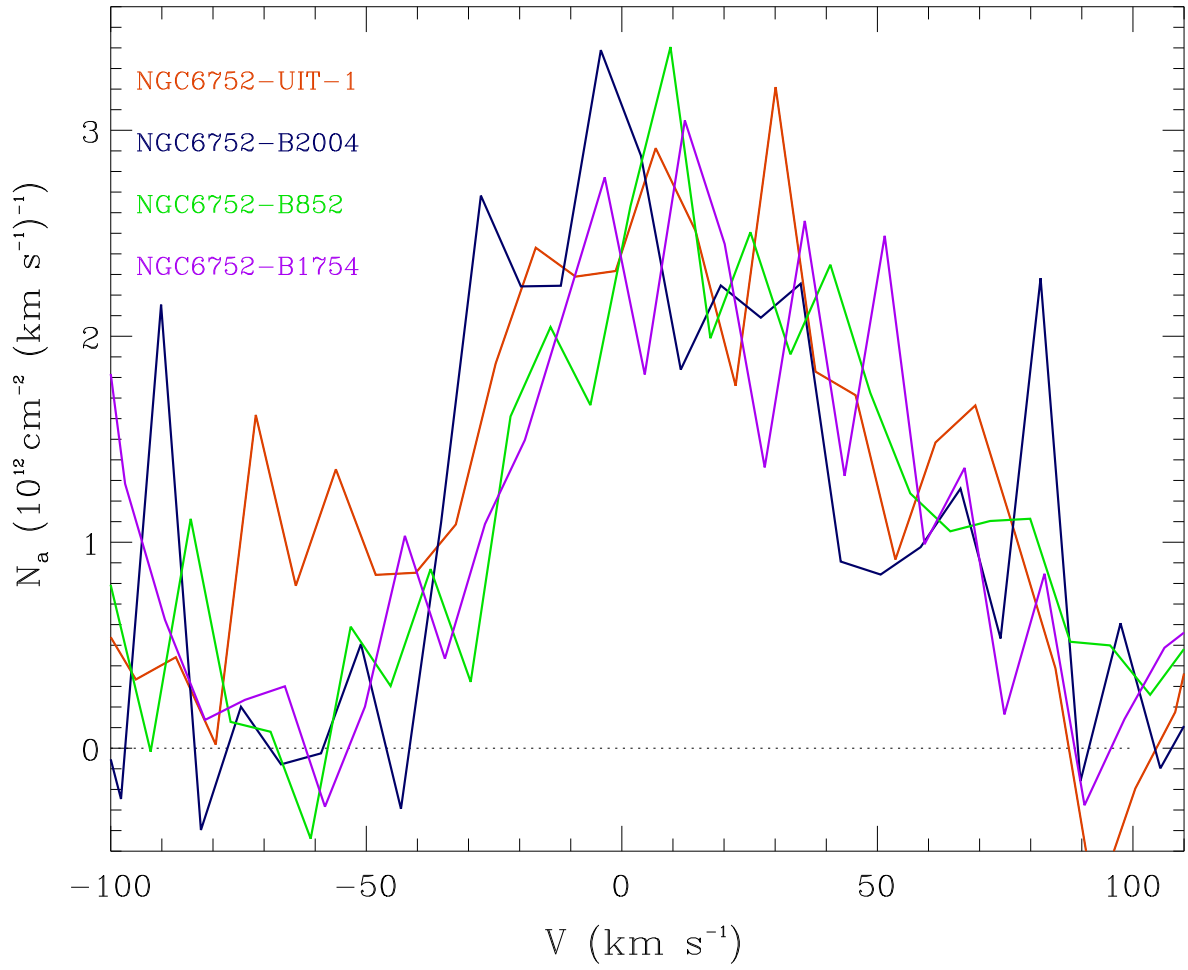Fig. 4.— Comparison of the apparent column density of O VI λ1032 and O VI λ1038 for each sight lines.

Fig. 5.— Comparison of the apparent column density of O VI λ1038 toward each sight lines.